



# Rogue events in the group velocity horizon

SUBJECT AREAS:  
PHYSICS  
OPTICAL PHYSICS  
NONLINEAR OPTICS  
SUPERCONTINUUM  
GENERATION

Ayhan Demircan<sup>1</sup>, Shalva Amiranashvili<sup>2</sup>, Carsten Brée<sup>2</sup>, Christoph Mahnke<sup>3</sup>, Fedor Mitschke<sup>3</sup> & Günter Steinmeyer<sup>4,5</sup>

<sup>1</sup>Invalidenstraße 114, 10115 Berlin, Germany, <sup>2</sup>Weierstrass Institute for Applied Analysis and Stochastics, 10117 Berlin, Germany, <sup>3</sup>Institute for Physics, University of Rostock, 18055 Rostock, Germany, <sup>4</sup>Max Born Institute for Nonlinear Optics and Short Pulse Spectroscopy, 12489 Berlin, Germany, <sup>5</sup>Optoelectronics Research Centre, Tampere University of Technology, 33101 Tampere, Finland.

Received  
2 July 2012

Accepted  
29 October 2012

Published  
14 November 2012

Correspondence and  
requests for materials  
should be addressed to  
A.D. (ayhan.  
demircan@gmx.de)

The concept of rogue waves arises from a mysterious and potentially calamitous phenomenon of oceanic surfaces. There is mounting evidence that they are actually commonplace in a variety of different physical settings. A set of defining criteria has been advanced; this set is of great generality and therefore applicable to a wide class of systems. The question arises naturally whether there are generic mechanisms responsible for extreme events in different systems. Here we argue that under suitable circumstances nonlinear interaction between weak and strong waves results in intermittent giant waves with all the signatures of rogue waves. To obtain these circumstances only a few basic conditions must be met. Then reflection of waves at the so-called group-velocity horizon occurs. The connection between rogue waves and event horizons, seemingly unrelated physical phenomena, is identified as a feature common in many different physical systems.

The appearance of rare but extremely powerful optical waves in nonlinear fiber supercontinua<sup>1–3</sup> provided a surprising laboratory analogy of rogue waves<sup>4,5</sup>. These laboratory experiments have opened up new possibilities for the investigation of this mysterious and severely destructive phenomenon observed in oceans worldwide. Characteristic signatures of ocean rogue waves can also be found in a variety of different classical and quantum systems. Outside the context of optics, analogies have been shown for matter waves<sup>6</sup>, superfluidity<sup>7</sup>, filaments<sup>8</sup>, and others. The concept of rogue waves has now evolved into an autonomous topic in science<sup>9</sup>, in particular as the dramatic concentration of energy into giant waves exhibits a high potential for various applications<sup>10</sup>. While there is now growing consent on a set of unified defining criteria for rogue waves across various physical systems, explanations for the appearance of giant waves often rely on nonlinear mechanisms peculiar to the individual case, e.g., the Raman effect in optics. Given the ubiquity of rogue waves in physics, it appears intriguing to search for common prerequisites and mechanisms across the systems. It would indeed be interesting if a mechanism could be identified that generates rogue waves in more than just one physical system. That would help to move from a purely phenomenological observation of similarities towards a deeper understanding of the underlying physical mechanisms. Possible ingredients for such mechanism are a dispersive and a nonlinear contribution to the wave velocity. Dispersion, i.e., a non-trivial dependence of propagation speed on the wave vector, appears in essentially all wave-supporting physical systems, which typically also exhibit a dependence of propagation speed on wave amplitude.

As a definition of rogue waves three criteria have been put forward<sup>9</sup>: i) The amplitude or corresponding characteristic of a rogue wave is at least twice the average amplitude<sup>11</sup>. ii) The phenomenon is localized and unpredictable in the sense that the wave seems to “appear from nowhere and disappear without a trace”<sup>12</sup>. iii) The statistical distribution of the wave crests reveals a non-Gaussian heavy tail, i.e., extreme events are significantly more frequent than typically anticipated.

Beyond these criteria, an underlying modulation instability is regarded to be connected to the formation of rogue waves. Modulation instabilities require dispersion and a nonlinearity of the propagation speed, i.e., exactly those conditions that have been identified for rogue-wave supporting systems. Moreover, these same effects constitute the basis for an enhanced interaction between light pulses, enabling an all-optical reflection process by means of the familiar cross-phase modulation<sup>13</sup>. The basic idea behind this interaction process is that an intense light pulse traveling down a nonlinear optical fiber creates a propagating front at which the propagation speed suddenly changes. If a co-propagating second pulse with nearly identical group velocity approaches that front, that pulse does not pass through the other pulse but gets reflected. Suitable conditions include an interaction

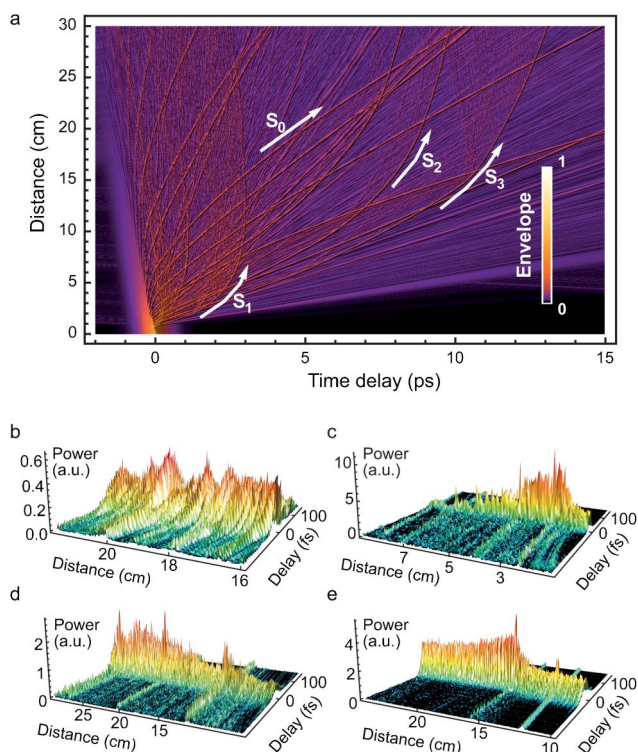


**Figure 1** | (a) Temporal evolution during propagation of a higher-order soliton injected close to the fiber zero dispersion frequency. Parameters are typical for a supercontinuum generation process. Arrows mark an unaffected soliton (S0) and three accelerated solitons (S1)–(S3). (b) Three-dimensional plot in the comoving frame of an unaffected fundamental soliton (S0). (c)–(e) Same for intermittent giant solitons (S1)–(S3).

length of some extent for a dispersive wave and a soliton, but these prerequisites are easily met when the fiber dispersion profile exhibits a zero dispersion wavelength. The reflection process is at the heart of the so-called optical event horizon<sup>14–17</sup>, and it is accompanied by generation of new frequencies<sup>18–21</sup>. Similar concepts in optics have been demonstrated earlier, both theoretically<sup>22</sup> and experimentally<sup>23</sup> in a fiber Bragg grating. Moreover, application of the event horizon concept can be found in recent work on two-wave collisions<sup>24,25</sup>. The reflection process at a group velocity horizon is not restricted to optical pulses in nonlinear media but can be found in many other systems<sup>17,26–28</sup>, including water surface waves<sup>29</sup> where it is known as wave blocking<sup>30</sup>.

It has been demonstrated<sup>31</sup> that the reflection process does not only affect the weak pulse, but also leads to a manipulation of the intense pulse. This observation indicates that the impact of tiny waves on strong pulses must be taken into account to properly describe rogue wave formation. In the following we will discuss that the reflection process at a group velocity horizon naturally appears in the supercontinuum generation process and has the ability to create extreme but rare events, i.e., rogue waves.

## Results

For the investigation of rogue wave formation in a supercontinuum generation process, we numerically simulated the propagation of an intense optical pulse launched into the anomalous dispersion regime of a photonic crystal fiber. We disregard higher-order effects specific for optics in order to maintain the generality of our argument. Moreover, we neglect the Raman effect. While this effect indeed plays an important role for ultrashort pulse propagation and the observations of optical rogue waves<sup>1</sup>, it is also a nonlinearity very specific to optics, and it has been shown not to be strictly required for rogue

wave formation in this system<sup>32</sup>. It should be noted that we do not exclude the possible existence of a second, Raman-based, rogue wave formation mechanism in optics. Parameters are detailed in the ‘Methods’ section; they correspond to the regime where the complex scenario of supercontinuum generation<sup>33</sup> takes place and where rogue waves are observed<sup>1,2,32,34</sup>.

Figure 1(a) displays the typical temporal dynamics of soliton fission<sup>35</sup>. Several fundamental solitons are ejected. These solitons are ultrashort pulses of different duration (but all in the femtosecond regime) and different peak powers. Their trajectories appear as pronounced lines which clearly stand out from the background. The different slopes of the trajectories indicate different velocities, on account of different center frequencies (not shown in Fig. 1) and the frequency dependence of the group velocity. This way, the ensemble of solitons is spread out in time. If the solitons remained undisturbed, one would expect them to propagate along straight trajectories in Fig. 1(a). The fission process also generates less intense phase-matched dispersive waves in the normal dispersion regime<sup>35</sup>, which propagate with a velocity close to that of the solitons. These dispersive waves eventually form a low-level radiation background across the  $t$ - $z$  plane. As we deliberately excluded Raman scattering in our analysis, we might expect that the group velocity of solitons is constant except in isolated places where soliton-soliton scattering processes occur. Indeed, inspection of Fig. 1 reveals several such characteristic crossings of soliton trajectories in the  $t$ - $z$  plane. However, we also find that the trajectories of the solitons S1–S3 do not appear to be ruled by isolated scattering events. The parabolic curve of the soliton trajectories indicates their constant acceleration.

A close inspection of the solitons S0–S3 in Fig. 1(a)–(e) already reveals essential signatures of event horizons. Consider S3, for example. The trajectory curves suddenly upward near  $z = 15$  cm, where weaker traces of background radiation hit the soliton and bounce off it. At the same position, the soliton peak power experiences a sudden increase by more than a factor two [Fig. 1(e)]. In fact, in all cases shown in Fig. 1(b)–(e) there is a strong correlation between the appearance of curved soliton trajectories and sudden changes of peak power. In contrast, S0 follows a nearly linear trajectory and, correspondingly, shows no comparable increase. This kind of power enhancing interaction represents an inherent phenomenon in the supercontinuum generation and can also be observed in presence of higher-order effects such as the Raman effect<sup>36–38</sup>.

This more than twofold increase of peak power [Fig. 1(c)–(e)] already fulfills the first criterion for rogue waves. The actual amount of increase is correlated to the amount of acceleration and is apparently determined by (unpredictable) details of the collision. Similarly, the subsequent decrease of peak powers can be fast (S1) or slow (S3), again with sensitive dependence on initial conditions. This shows that the second criterion for rogue waves, unpredictable appearance and disappearance, is also fulfilled. We will turn to the third rogue wave criterion (skewed statistics) below.

We have performed numerous simulations with different soliton numbers and consistently observe the above-discussed behavior whenever soliton fission triggers the generation of supercontinuum. With increasing peak power the number of temporarily existing giant solitons increases. It is important to note that the supercontinuum generation process as modeled here is fully capable of producing a modulation instability<sup>33,39</sup>. However, at least with the rather moderate powers assumed here, this instability only manifests itself via certain periodic spikes in the initial  $\approx 0.5$  cm propagation length. It is known that the modulation instability may initiate the underlying soliton fission process<sup>40</sup>, but is not a necessary prerequisite for the fission. For the case at hand, we conclude that this process is of little importance to the subsequent giant wave generation.

For a thorough understanding of the dynamics, let us further consider example S3. To follow its fate, we extracted all soliton parameters and show them separately in Fig. 2. Its trajectory exhibits a

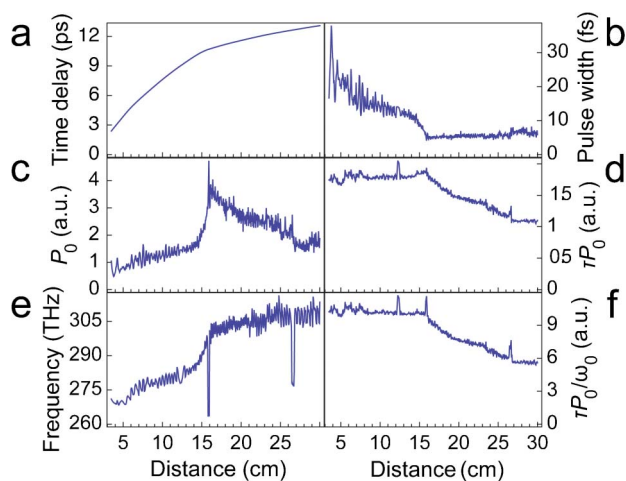


**Figure 2** | Evolution of the isolated soliton parameters: (a) trajectory, (b) pulse width, (c) peak intensity, (d) energy, (e) carrier frequency, (f) photon number.

conspicuous bend at  $z \approx 14$  cm, which immediately manifests itself in the curvature of the time delay curve of Fig. 2(a). Yet, at the very same position, nearly all other soliton parameters also experience a pronounced change in the range from 15 to 16 cm. The pulse duration is reduced [Fig. 2(b)] while the peak power increases [Fig. 2(c)]. Moreover, the carrier frequency is upshifted [Fig. 2(e)], which results in a change of the group velocity. We therefore conclude that along its travel along trajectory S3, the wave increases significantly in power and becomes a giant wave. Nevertheless, the pulse energy [Fig. 2(d)] rises only minimally, and the photon number [Fig. 2(f)] remains nearly constant all the way up to  $z = 16$  cm. This finding indicates that the interaction process between continuum background and soliton is mainly a reshaping process. A little further down the fiber, at  $z \approx 16$  cm, the soliton reaches the zero-dispersion frequency (305 THz) of the fiber. With parts of the spectrum crossing into the normal dispersion regime, both energy and photon number drop,

and the peak power begins to decrease. This reduction is accompanied by dispersive waves radiated off and eventually leads to a quick disappearance of the giant wave.

In the presence of the clutter of several solitons on a wide and varied background of radiation, it is difficult to irrefutably identify cause and effect of the dynamics of each individual soliton. We therefore ventured to isolate a representative soliton and selected segments of the dispersive waves in Fig. 1(a) right at the onset of the trajectory curvature, such that a deterministic interpretation of the rogue wave formation decoupled from the supercontinuum generation process becomes viable. To this end we numerically launch a soliton with properties copied from the case of S2 [Fig. 1(c)] (center frequency  $\nu_s = 268.5$  THz, width 30 fs FWHM) together with a temporal segment (width 118 fs) of dispersive waves near the velocity-matched frequency of  $\nu_d = 549$  THz. The result is displayed in Fig. 3, with panels (a) and (c) showing the temporal and spectral evolution, respectively. For the sake of greater clarity, the temporal coordinate is shifted at a constant rate with respect to that in Fig. 1 so that the dominant constant contribution to the group velocity is effectively removed. Given the choice of the reference frame in Fig. 3(a), any deviation of the soliton trajectory from a straight line parallel to the axis can only result from nonlinear interaction with the injected continuum radiation. It is obvious that interaction takes place upon collision, and it is also plain that the soliton gets reshaped, with a change of its peak power upon each interaction. What we actually see in Fig. 3(a) is the optical analogue to an event horizon. Its origin is the Kerr-mediated refractive index modulation by the soliton which the radiation runs into. The radiation then either stays close to the soliton or escapes by shifting its frequency, with either option implying strong interaction between both.

These processes are completely elastic, and they induce a mutual shift of optical frequencies. With the photon number of the soliton practically conserved, the soliton blue shift accordingly causes a mild increase of its energy [Fig. 3(c)]. The shifted soliton also experiences a considerably smaller  $\beta_2$  [Fig. 3(b)]. Considering that the energy of a soliton is expressed through the peak power  $P_0$  and  $\beta_2$  as  $E = 2\sqrt{P_0|\beta_2|/\gamma}$ , the decrease of  $\beta_2$  cannot be compensated by a

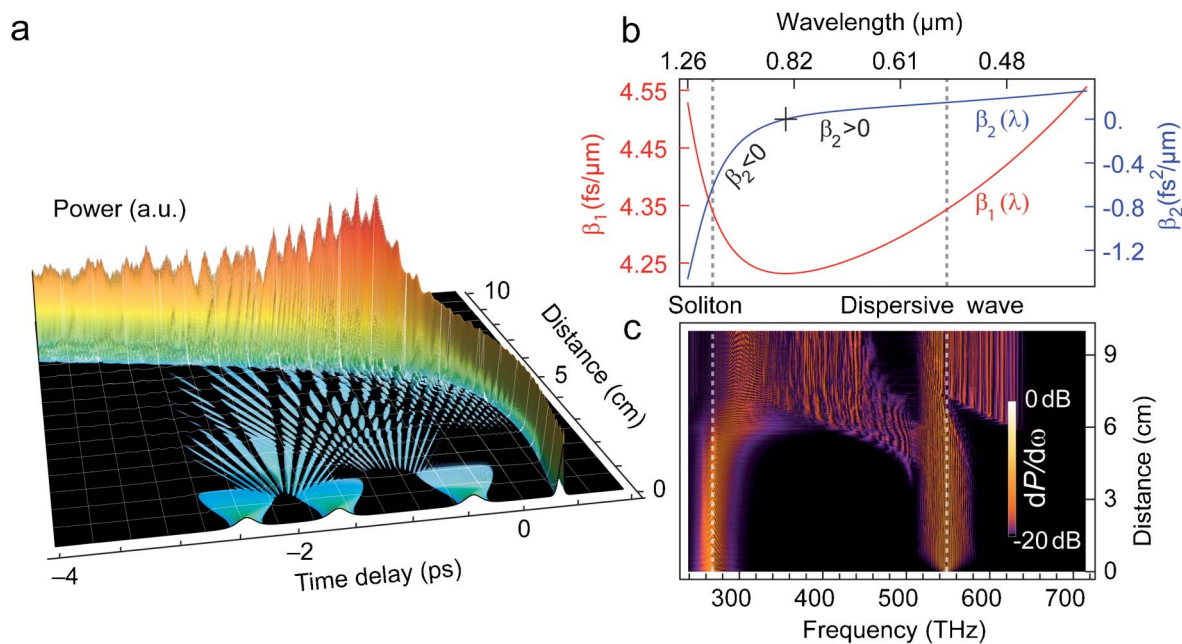


**Figure 3** | (a) Three dimensional time domain evolution along the fiber representing the isolated trajectory of a fundamental soliton. Acceleration results from a cascaded scattering with three dispersive waves. (b) Concave group delay  $\beta_1 = \beta'(\omega)$  and related group-velocity dispersion  $\beta_2 = \beta''(\omega)$ , with the extracted wavelengths for the fundamental soliton at  $\lambda_s = 1030$  nm and a dispersive pulse at  $\lambda_d = 614$  nm (dashed line). (c) Spectral evolution of the deterministic rogue wave formation process.

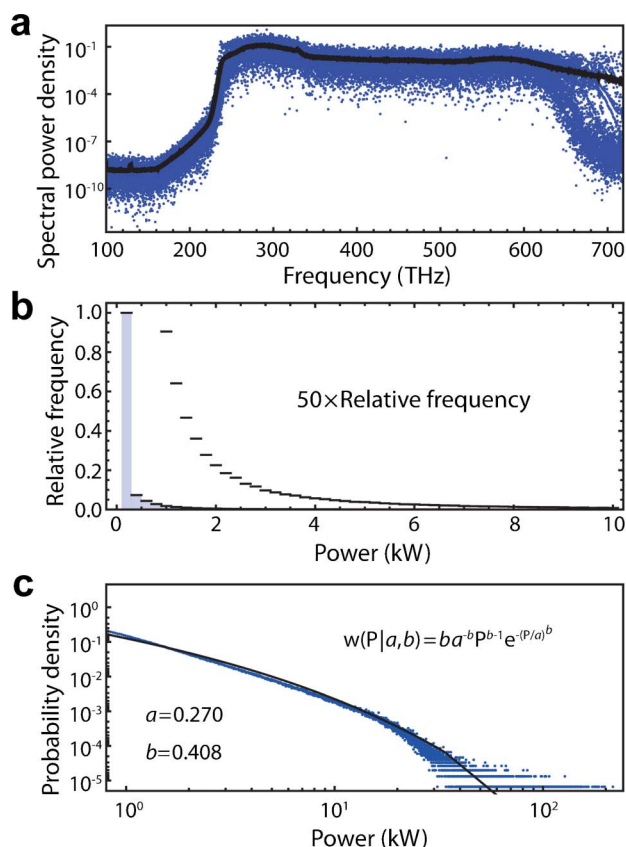


**Figure 4** | (a) Single-shot and mean spectrum at the end of the fiber,  $z = 8$  cm. (b) Histogram of the peak power frequency distribution. (c) Statistical distribution on a log-log scale with a fit to a Weibull distribution.

reduction of  $E$  because  $E$  also grows. As  $\gamma$  does not vary appreciably, consequently,  $P_0$  is forced to grow massively. Like in the “optical push broom” effect<sup>22,23</sup> the enhanced cross phase modulation by a group-velocity horizon is used for a pulse compression, but the mechanism described here is markedly different from schemes where a strong pulse modifies a weak probe pulse without getting affected itself. Instead, a significant manipulation of a strong pulse is induced by much weaker pulses here.

This mechanism dictated by the intricate dependence between soliton parameters clearly explains the generation of giant waves apparently coming from nowhere. Figure 3(c) shows the spectral evolution during the reflection process. The central frequency of the soliton is shifted toward the zero dispersion frequency, and its spectrum is broadened due to the temporal compression. Approaching the zero dispersion frequency, part of its spectral power begins to overlap with the normal dispersion regime and is lost to dispersive radiation. This overlap leads to the destruction of the giant wave, and a soliton remains with lower peak intensity but nearly the same pulse width. Also, the strength of the destruction process may vary greatly, depending on the strength of the interaction between the soliton and the dispersive waves. The described behavior unveils two important points. The generation and destruction of the giant wave do not have to be based on the same mechanism, and their overall description does not have to rely on a closed solution. In any event, while fundamental solitons are often excluded as possible candidates for rogue waves due to their stability, we conclude that they may play an important role in rogue wave phenomena after all.

All features observed in the supercontinuum generation can clearly be reproduced by the controlled interaction scenario between the isolated soliton and dispersive waves. We repeated these simulations with several segments of the continuum with enhanced energy,

to test whether even higher soliton peak powers can be obtained. We observe that the stronger the induced frequency shift is, the faster the giant soliton builds up and then vanishes again. By judicious insertion of dispersive waves, both the appearance and disappearance as well as the extent of the peak power enhancement can be controlled. Our discussion also demonstrates that modulation instability is irrelevant for this deterministic mechanism of rogue wave generation.

We now turn to the third criterion for rogue waves, its skewed statistical distribution. We generated a total of 4000 realizations of supercontinua, using different noise seeds, shown in Fig. 4(a) together with the average spectrum. Clearly, shot-to-shot variations are considerable. Figure 4(b) displays the histogram of pulse intensities extracted from the time series. This histogram displays the typical heavy-tailed figure-L shape which is characteristic for rare-but-extreme events. Figure 4(c) shows the same data set on a log-log scale. It is obvious that it fits very well to a Weibull distribution. We emphasize that these data were obtained without spectral filtering of the time series<sup>41</sup>. While some published results involved such filtering of noisy supercontinuum data, it is now understood that filtering may produce misleading results. This discussion makes it clear that the third criterion for rogue waves – its skewed statistics – is fulfilled, too.

Rogue waves, subject to non-Gaussian statistics, have already been shown to appear in the fiber supercontinuum generation both with and without Raman frequency shift<sup>32</sup>. The emergence of a single “champion” soliton due to multiple collisions between optical solitons was previously discussed as one possible mechanism behind rogue wave formation. This reasoning follows the idea that large solitons may extract energy from a turbulent soliton ensemble described by the Nonlinear Schrödinger Equation<sup>42</sup>. However, a multitude of collisions between solitons is required for such a growth. In contrast, in our system giant solitons are observed before a sizeable number of suitable collisions occurs. Therefore, the nature of the newly observed continuum-soliton scattering processes is markedly different from soliton-soliton scattering. As continuum radiation quickly disperses there will always be temporal slices of the dispersive waves that effectively copropagate with a given soliton, making mutual extended interaction much more likely than the appearance of a sufficient number of soliton-soliton processes.

## Discussion

We have demonstrated a mechanism for rogue wave formation which relies only on two ingredients, a dispersive and a nonlinear contribution to the wave velocity. This minimal set of requirements can rightfully be expected to exist in a wide class of physical systems. The rogue waves discussed here are not closed solutions of the wave equation like, e.g., the Akhmediev breather<sup>43</sup> or the Peregrine soliton<sup>44</sup>. Instead, the class of rogue waves discussed here emerges from interaction between the continuum background and solitons. Moreover, the mechanism is completely deterministic, which gives rise to some interesting thoughts:

How can this concept be exploited in various physical systems to control the power of pulses? If one knew all key parameters, could one restrain the unpredictability inherent in the process? Ultimately, could one suppress the emergence of giant waves? And how would this apply to immensely complex systems like ocean surface waves? We believe that the discovery of this mechanism of rogue wave formation will enable a deeper understanding of this fascinating yet possibly devastating phenomenon.

## Methods

**Propagation model.** For our numerics, we use a non-envelope propagation model for ultrashort pulses in a nonlinear waveguide<sup>45</sup>. To trace the real-valued optical field  $E(z, t)$  we introduce a complex-valued  $\mathcal{E}(z, t)$  such that in the frequency domain  $\mathcal{E}_\omega(z) = E_\omega(z) - i\partial_z E_\omega(z)/|\beta(\omega)|$ . Note that  $E = \text{Re}(\mathcal{E})$  and that the positive (negative) frequency part of  $\mathcal{E}(z, t)$  corresponds to the forward (backward) waves. This enables us to keep only the Kerr effect as a nonlinearity and to omit higher



harmonic generation, which is only a distraction here. The basic propagation equation for  $\mathcal{E}(z, t)$  reads

$$i\partial_z \mathcal{E}_\omega + |\beta(\omega)| \mathcal{E}_\omega + \frac{3\omega^2 \chi^{(3)}}{8c^2 |\beta(\omega)|} (|\mathcal{E}|^2 \mathcal{E})_\omega = 0. \quad (1)$$

Parameters  $c$ ,  $\chi^{(3)}$ , and  $\beta(\omega)$  are the speed of light, the third-order nonlinear susceptibility, and the propagation constant, respectively. For unidirectional propagation regime  $\varepsilon(z, t)$  is identical to the analytic signal  $\mathcal{E}(z, t) = 2 \sum_{\omega > 0} E_\omega(z) e^{-i\omega t}$ .

Our description of the optical field is then equivalent to using the forward Maxwell equation<sup>35</sup>, but with the benefit of a clear separation from third harmonic generation. Note that for the sake of universality we also neglect the Raman effect. The latter clearly affects both pulse propagation and generation of optical rogue waves<sup>1</sup>, but it represents a nonlinear process quite specific to optics, and it is neither an inevitable necessity for rogue wave formation, nor of much importance for the main concept of a group velocity horizon.

If the slowly-varying envelope description with respect to a suitable carrier frequency applies, Eq. (1) reduces to the standard nonlinear Schrödinger equation, and the absolute magnitude of  $\mathcal{E}(z, t)$  is the same as that of the envelope.

Equation (1) is subject to the conservation laws

$$I_1 = \sum_{\omega} \frac{n(\omega)}{\omega} |\mathcal{E}_\omega|^2, \quad I_2 = \sum_{\omega} n(\omega) |\mathcal{E}_\omega|^2, \quad (2)$$

where  $n(\omega)$  is the frequency-dependent refractive index, and  $I_{1,2}$  are finite quantities proportional to the time-averaged photon flux and power, respectively<sup>45</sup>. Our approach correctly models nonlinear processes between waves of different frequencies such as four-wave mixing and cross phase modulation between solitons and dispersive waves, and between individual solitons. In the following, we consider a typical single-mode photonic crystal fiber with a single zero-dispersion frequency similar to the fiber used in Ref. (3).

For our numerical work we use a de-aliased pseudospectral method originating from computational fluid dynamics<sup>46</sup>. The conventional split-step Fourier approach either requires very small space steps or lacks precision for a few-cycle optical pulse and relatively long propagation distance, such that the integrals of motion are not conserved. However, numerical implementation of a Runge-Kutta integration scheme of 8<sup>th</sup> order with adaptive step-size control for the integration of the linear and nonlinear part in the frequency domain allows calculations in a very efficient and accurate manner. Considering ultrashort optical pulses with the carrier frequencies of several hundreds THz, we use at least  $\Delta t = 0.6$  fs. Depending on the initial pulse width we use  $2^{17}$  or  $2^{18}$  discretization points for a periodic time window  $T = 5$  ps and  $T = 10$  ps, respectively. Several test calculations with resolution increased to  $2^{19}$  points were performed, but this turned out to be unnecessary.

We simulated the propagation in the anomalous dispersion regime of a photonic crystal fiber close to its zero dispersion wavelength  $\lambda_{ZDW} = 842$  nm. Pulse parameters are: center wavelength  $\lambda_c = 897$  nm, full width at half maximum FWHM = 265 fs, and peak power of 22 kW. The fiber nonlinearity parameter was  $\gamma = 0.1 \text{ W}^{-1} \text{ m}^{-1}$ . The dispersion was as shown in Fig. 3(b); in particular, parameter  $\beta_2 = -0.053 \text{ fs}^2/\mu\text{m}$  is required to estimate the soliton order<sup>33</sup>, which for the quoted pulses is  $N \approx 38$ .

As a final sanity check of our method, we performed comparative simulations for the supercontinuum generation in Fig. 1(a) with the generalized Schrödinger equation, both with a split-step and a Runge-Kutta scheme. This is a well-established technique, but by its very nature it is not capable of making the distinction of energy and photon number, and thus of a correct assessment of the energy transfer described above. However, we could convince ourselves that the propagation dynamics is virtually the same as with our more elaborate ansatz.

1. Solli, D. R., Ropers, C., Koonath, P. & Jalali, B. Optical rogue waves. *Nature* **450**, 1054–1057 (2007).
2. Mussot *et al.* Observation of extreme temporal events in CW-pumped supercontinuum. *Opt. Exp.* **17**, 17010–17015 (2009).
3. Dudley, J. M., Genty, G. & Eggleton, B. J. Harnessing and control of optical rogue waves in supercontinuum generation. *Opt. Exp.* **16**, 3644–3651 (2008).
4. Dysthe, K., Krogstad, H. E. & Müller, P. Oceanic Rogue Waves. *Annu. Rev. Fluid Mech.* **40**, 287–310 (2008).
5. Khariif, C. & Pelinovsky, E. Physical mechanisms of the rogue wave phenomenon. *Eur. J. Mech.* **22**, 603–634 (2003).
6. Bludov, Y. V., Konotop, V. V. & Akhmediev, N. Matter rogue waves. *Phys. Rev. A* **80**, 033610 (2009).
7. Ganshin, A. N., Efimov, V. B., Kolmakov, G. V., Mezhev-Deglin, L. P. & McClintock, P. V. E. Observation of an Inverse Energy Cascade in Developed Acoustic Turbulence in Superfluid Helium. *Phys. Rev. Lett.* **101**, 065303 (2008).
8. Majus, D., Jukna, V., Valiulis, G., Faccio, D. & Dubietis, A. Spatiotemporal rogue events in femtosecond filamentation. *Phys. Rev. A* **83**, 025802 (2011).
9. Akhmediev, N. & Pelinovsky, E. Editorial – Introductory remarks on Discussion and Debate: Rogue waves — towards a unifying concept? *Eur. Phys. J. Special Topics* **185**, 1–4 (2010).

10. Akhmediev, N., Soto-Crespo, J. M. & Ankiewicz, A. How to excite a rogue wave. *Phys. Rev. A* **80**, 043818 (2009).
11. Janssen, P. A. E. M. Nonlinear Four-Wave Interactions and Freak Waves. *J. Phys. Oceanogr.* **33**, 863–884 (2003).
12. Akhmediev, N., Ankiewicz, A. & Taki, M. N. Waves That Appear from Nowhere and Disappear without a Trace. *Phys. Lett. A* **373**, 675–678 (2009).
13. Agrawal, G. *Nonlinear Fiber Optics*. (Academic Press, San Diego, 2001).
14. Philbin, T. G. *et al.* U. Fiber-Optical Analog of the Event Horizon. *Science* **319**, 1367–1370 (2008).
15. Faccio, D. Laser pulse analogues of gravity and analogue Hawking radiation. *Cont. Phys.* **1**, 1–16 (2012).
16. Choudhary, A. & König, F. Efficient frequency shifting of dispersive waves at solitons. *Opt. Exp.* **20**, 5538–5546 (2012).
17. Belgiorno, F. *et al.* Hawking Radiation from Ultrashort Laser Pulse Filaments. *Phys. Rev. Lett.* **105**, 203901 (2010).
18. Yulin, A. V., Skryabin, D. V. & Russell, P. Four-wave mixing of linear waves and solitons in fibers with higher-order dispersion. *Opt. Lett.* **29**, 2411–2413 (2004).
19. Efimov, A. *et al.* Interaction of an Optical Soliton with a Dispersive Wave. *Phys. Rev. Lett.* **95**, 213902 (2005).
20. Gorbach, A. V. & Skryabin, D. V. Light trapping in gravity-like potentials and expansion of supercontinuum spectra in photonic-crystal fibres. *Nature Photon.* **1**, 653–657 (2007).
21. Gorbach, A. V. & Skryabin, D. V. Bouncing of a dispersive pulse on an accelerating soliton and stepwise frequency conversion in optical fibers. *Opt. Exp.* **15**, 14560–14565 (2007).
22. De Sterke, C. M. Optical push broom. *Opt. Lett.* **17**, 914–916 (1992).
23. Broderick, N. G. R., Taverner, D., Richardson, D. J., Ibsen, M. & Laming, R. I. Optical Pulse Compression in Fiber Bragg Gratings. *Phys. Rev. Lett.* **79**, 4566–4569 (1997).
24. Rosanov, N. Transformation of electromagnetic radiation at moving inhomogeneities of a medium. *JETP Lett.* **88**, 501–504 (2008).
25. Lobanov, V. E. & Sukhorukov, A. P. Total reflection, frequency, and velocity tuning in optical pulse collision in nonlinear dispersive media. *Phys. Rev. A* **82**, 033809 (2010).
26. Novello, M., Visser, M. & Volovik, G. (eds.) *Artificial Black Holes*. (World Scientific, New Jersey, London, Singapore, Hong Kong, 2002).
27. Garay, L. J., Anglin, J. R., Cirac, J. I. & Zoller, P. Sonic Analog of Gravitational Black Holes in Bose-Einstein Condensates. *Phys. Rev. Lett.* **85**, 4643–4647 (2000).
28. Jacobson, T. A. & Volovik, G. E. Event horizons and ergoregions in <sup>3</sup>He. *Phys. Rev. D* **58**, 064021 (1998).
29. Rousseaux, G., Mathis, C., Maïssa, P., Philbin, T. G. & Leonhardt, U. Observation of negative-frequency waves in a water tank: a classical analogue to the Hawking effect? *New J. Phys.* **10**, 053015 (2008).
30. Smith, R. Reflection of short gravity waves on a non-uniform current. *Math. Proc. Camb. Phil. Soc.* **78**, 517–525 (1975).
31. Demircan, A., Amiranashvili, Sh. & Steinmeyer, G. Controlling light by light with an optical event horizon. *Phys. Rev. Lett.* **106**, 163901 (2011).
32. Genty, G. *et al.* Collisions and turbulence in optical rogue wave formation. *Phys. Lett. A* **374**, 989–996 (2010).
33. Dudley, J. M., Genty, G. & Coen, S. Supercontinuum Generation in Photonic Crystal Fiber. *Rev. Mod. Phys.* **78**, 1135 (2006).
34. Kibler, B., Finot, C. & Dudley, J. M. Soliton and rogue wave statistics in supercontinuum generation in photonic crystal fiber with two zero dispersion wavelengths. *Eur. Phys. J. Special Topics* **173**, 289–295 (2009).
35. Husakou, A. V. & Herrmann, J. Supercontinuum Generation of Higher-Order Solitons by Fission in Photonic Crystal Fibers. *Phys. Rev. Lett.* **87**, 203901 (2001).
36. Robertson, S. & Leonhardt, U. Frequency shifting at fiber-optical event horizons: The effect of Raman deceleration. *Phys. Rev. A* **81**, 063835 (2010).
37. Driben, R., Mitschke, D. & Zhavoronkov, N. Cascaded interactions between Raman induced solitons and dispersive waves in photonic crystal fibers at the advanced stage of supercontinuum generation. *Opt. Exp.* **18**, 25993–25998 (2010).
38. Skryabin, D. V. & Gorbach, A. V. Colloquium: Looking at a soliton through the prism of optical supercontinuum. *Rev. Mod. Phys.* **82**, 1287–1299 (2010).
39. Demircan, A. & Bandelow, U. Supercontinuum generation by the modulation instability. *Opt. Commun.* **244**, 181–185 (2005).
40. Demircan, A. & Bandelow, U. Analysis of the interplay between soliton fission and modulation instability in supercontinuum generation. *Appl. Phys. B* **86**, 31–39 (2007).
41. Erkintalo, M., Genty, G. & Dudley, J. M. On the statistical interpretation of optical rogue waves. *Eur. Phys. J. Special Topics* **185**, 135–144 (2010).
42. Zakharov, V. E., Pushkarev, E., Shvets, V. F. & Yan'kov, V. V. Soliton turbulence in nonintegrable wave systems. *JETP Lett.* **48**, 83–87 (1988).
43. Akhmediev, N., Ankiewicz, A. & Soto-Crespo, J. M. Rogue waves and rational solutions of the nonlinear Schrödinger equation. *Phys. Rev. E* **80**, 026601 (2009).
44. Kibler, B. *et al.* The Peregrine soliton in nonlinear fibre optics. *Nature Physics* **6**, 790–795 (2010).
45. Amiranashvili, Sh. & Demircan, A. Hamiltonian structure of propagation equations for ultrashort optical pulses. *Phys. Rev. A* **82**, 013812 (2010).



46. Canuto, C., Hussaini, M. Y., Quarteroni, A. & Zang, T. A. Spectral methods: Fundamentals in single domains. Springer, Berlin, 3<sup>rd</sup> edition, (2006).

## Acknowledgements

The following support is gratefully acknowledged: S.A. is supported by DFG Research Center MATHEON (project D 14), G.S. by the Academy of Finland (project grant 128844), and C.M. partially by DFG.

## Author contributions:

A.D. conceived the original idea and supervised the project throughout. A.D., C.B. and C.M. performed the numerical simulations of the propagation model developed by S.A. G.S., S.A. and C.B. performed the data analysis. A.D., G.S. and F.M. wrote the manuscript.

## Additional information

**Competing financial interests:** The authors declare no competing financial interests.

**License:** This work is licensed under a Creative Commons Attribution-NonCommercial-ShareAlike 3.0 Unported License. To view a copy of this license, visit <http://creativecommons.org/licenses/by-nc-sa/3.0/>

**How to cite this article:** Demircan, A. *et al.* Rogue events in the group velocity horizon. *Sci. Rep.* **2**, 850; DOI:10.1038/srep00850 (2012).